

OVERVIEW OF RELATIVISTIC HEAVY-ION PHYSICS

ITZHAK TSERRUYA

Dept. of Particle Physics, Weizmann Institute, Rehovot 76100, Israel
E-mail: Itzhak.Tserruya@weizmann.ac.il

Selected topics in the field of relativistic heavy-ion collisions are reviewed from the 15 year research programme at the SPS at CERN and the AGS at BNL, and from the first run of the Relativistic Heavy-Ion Collider at BNL.

1 Introduction

The Relativistic Heavy-Ion Collider (RHIC) at BNL started regular operation in the summer of year 2000 opening new horizons in the study of nuclear matter under extreme conditions of pressure, density and temperature. The primary scientific objective is the search for the phase transition associated with quark-gluon plasma formation and chiral symmetry restoration, predicted to occur under these conditions. According to QCD calculations on the lattice, with three light quark flavors (two degenerate u,d-quark masses and a strange quark), the phase transition should be of first order ¹.

In a very short, but extremely successful run with an integrated luminosity of only a few μb^{-1} , the four RHIC experiments have delivered an impressive amount of results offering a first glimpse at the physics of relativistic heavy-ion collisions at the highest energies achieved to date, $\sqrt{s_{NN}} = 130$ GeV, almost one order of magnitude larger than the highest energy of $\sqrt{s_{NN}} = 17.2$ GeV available at CERN. Together with that, the 15 years of relativistic heavy-ion physics at the CERN SPS and the BNL AGS have produced a wealth of very interesting and intriguing results in the quest for the quark-gluon plasma.

About a dozen of different experiments at the AGS and SPS and four experiments at RHIC are or have been involved in this endeavour covering a very broad range of observables which can be divided into two broad categories: (i) global and hadronic observables (transverse energy and charged particle distributions, p_t spectra, particle production rates, two-particle correlations, flow, etc.); they provide crucial information about the reaction dynamics and in particular about the size and properties of the final hadronic system at freeze-out i.e. when hadrons cease to interact. From their systematic studies, the picture of a chemically and thermally equilibrated hadronic system undergoing collective expansion has emerged, with freeze-out parameters (in the temperature vs. baryo-chemical potential plane) close to the expected phase transition boundaries. (ii) observables which have been proposed as signatures

for the phase transition: the most prominent ones for deconfinement are J/ψ suppression, real and virtual thermal photons and jet quenching. Low-mass dileptons and the ρ meson with its very short lifetime, are considered the best probes for the chiral symmetry restoration phase transition.

In the limited space of this paper it is not possible to do justice to the vast amount of available results ². A selection is therefore unavoidable and this paper is restricted to selected topics on (i) global observables where systematic comparisons are made from AGS up to RHIC energies, (ii) the observation of J/ψ suppression and excess emission of low-mass lepton pairs which are among the most notable results hinting at new physics from the SPS programme (results on these two topics are not yet available at RHIC as they require a much higher luminosity than achieved in the first year), and (iii) the suppression of high p_T hadrons which is one of the highlights of the first RHIC run pointing to new phenomena opening up at the high energies of RHIC.

2 Global Observables

Global observables, like multiplicity and transverse energy, provide very valuable information. Besides defining the collision geometry, they can be related to the initial energy density, e.g. using the well-known Bjorken relation ³, shed light into the mechanisms of particle production⁴ and provide constraints to the many models aiming at describing these collisions.

The charged particle rapidity density at mid-rapidity has been measured by the four RHIC experiments -BRAHMS, PHENIX, PHOBOS and STAR- with very good agreement among their results ⁵. For central Au-Au collisions at $\sqrt{s_{NN}} = 130$ GeV, the global average is $dN_{ch}/d\eta = 580 \pm 18$. For the transverse energy rapidity density there is only one measurement by PHENIX, with a value $dE_T/d\eta = 578_{-39}^{+26}$ GeV for the most central 2% of the inelastic cross section ⁶. Using the Bjorken formula ³ this translates into an initial energy density of $\epsilon = 5.0$ GeV/fm³ ^a. These values are 60-70% larger than the corresponding ones at the full SPS energy.

The energy dependence of the charged particle density $dN_{ch}/d\eta$, normalized per pair of participating nucleons ($N_{part}/2$), exhibits a boring logarithmic rise with $\sqrt{s_{NN}}$ from AGS up to RHIC energies, as shown in Fig. 1. However, the dependence is very different from the $p\bar{p}$ systematics also shown in Fig. 1. At $\sqrt{s_{NN}} = 200$ GeV, $\sim 65\%$ more particles per pair of participants are produced in Au-Au collisions than in $p\bar{p}$. I shall return to this point below. Note also that the large increase predicted by the HIJING

^aif one uses the canonical formation time $\tau = 1\text{fm}/c$. Much shorter formation times as advocated in saturation models ⁷ would result in energy densities as high as $\epsilon \simeq 20$ GeV/fm³.

model with jet quenching ⁴ (upper curve in Fig. 1) is not observed, and from $\sqrt{s_{NN}} = 130$ to 200 GeV the particle density increases only by 15% ⁵.

The centrality dependence of the charged particle density has been proposed as a sensitive tool to shed light on the particle production mechanism: whereas soft processes are believed to scale with the number of participants N_{part} , hard processes, expected to play a significant role as the energy increases, lead to a scaling with the number of binary collisions N_{bin} . Indeed, PHENIX and PHOBOS have reported an increase of $dN_{ch}/d\eta$ and $dE_T/d\eta$ strongly than linear with N_{part} (the PHENIX results are shown in Fig. 2 ⁸) and in the framework of models with these two components, like HIJING ^{7,9}, such an increase is interpreted as evidence of the contribution of hard processes to particle production ^b. This is to be contrasted to the results obtained at the SPS where WA98 reports a much weaker increase (also shown in Fig. 2) ¹¹ and WA97 an even weaker increase consistent within errors with proportionality between multiplicity and participants ¹². Both the PHENIX and the WA98 data, extrapolated to peripheral collisions, are in very good agreement with the $p\bar{p}$ result at the same \sqrt{s} derived from the UA5 data ¹⁴. The increased role of hard processes at higher energies and more central collisions would then be the explanation for the faster increase of particle production in A-A collisions compared to $p\bar{p}$ previously discussed in the context of Fig. 1. The importance of hard processes at RHIC energies is a very interesting issue which will be further discussed in this review.

More surprising is the behavior of the ratio $dE_T/d\eta/dN_{ch}/d\eta$, the average transverse energy per charged particle, shown in Fig. 3. This ratio is found to be independent of centrality and approximately equal to ~ 0.8 GeV. Within errors of the order of 10-20% this ratio is also independent of $\sqrt{s_{NN}}$ from AGS up to RHIC, implying a constant or a very moderate increase of the average p_T per particle. It is also interesting to note that UA1 quotes a very similar ratio at $\sqrt{s} = 200$ GeV ¹⁵. This seemingly universal behaviour of constant energy/particle is one of the most puzzling results. The increase in $dE_T/d\eta$

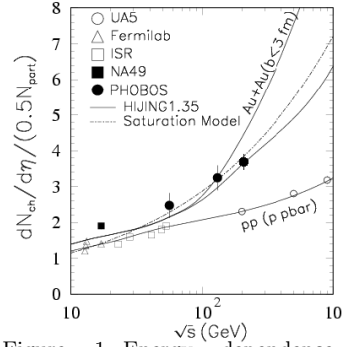


Figure 1. Energy dependence of charged particle density in central A-A and pp collisions ⁴.

^bThis is, however, not a unique interpretation. The centrality dependence results of PHENIX shown in Fig. 2 have also been explained with a model based on purely soft processes ¹⁰.

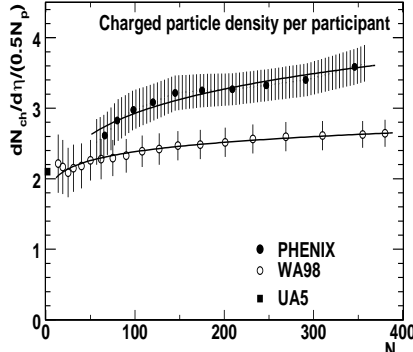


Figure 2. Centrality dependence of the charged particle density from PHENIX and WA98 ¹³.

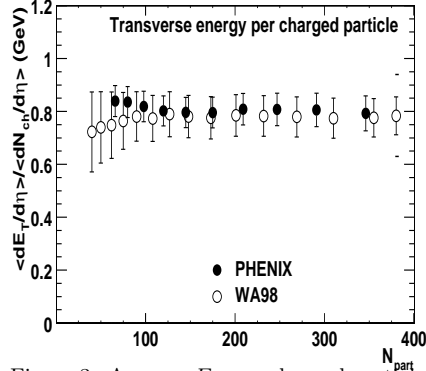


Figure 3. Average E_T per charged particle from PHENIX and WA98 ⁶.

with $\sqrt{s_{NN}}$ translates into an increase in the number of produced particles rather than in the production of particles with higher E_T .

3 Low-Mass e^+e^- Pairs

Dileptons and photons are since a long time emphasized as unique probes to study the dynamics of relativistic heavy-ion collisions ¹⁶. The interest stems from their relatively large mean free path. As a consequence, they can leave the interaction region without final state interaction, carrying information about the conditions and properties of the matter at the time of their production and in particular of the early stages of the collision when temperature and energy density have their largest values, i.e. when the conjectured deconfinement and chiral symmetry restoration phase transition has the best chance to occur.

The prominent topic of interest, both in dileptons and photons, is the identification of thermal radiation emitted from the collision system. This radiation should tell us the nature of the matter formed, a quark-gluon plasma (QGP) or a high-density hadron gas (HG). The physics potential of low-mass dileptons is further emphasized by their sensitivity to chiral symmetry restoration. The ρ -meson is the prime agent here. Due to its very short lifetime ($\tau = 1.3$ fm/c) compared to the typical fireball lifetime of ~ 10 fm/c at SPS energies, most of the ρ mesons decay inside the interaction region providing a unique opportunity to observe in-medium modifications of particle properties (mass and/or width) which might be linked to chiral symmetry restoration. The situation is different for the ω and ϕ mesons. Because of their much longer lifetimes they predominantly decay outside the interaction

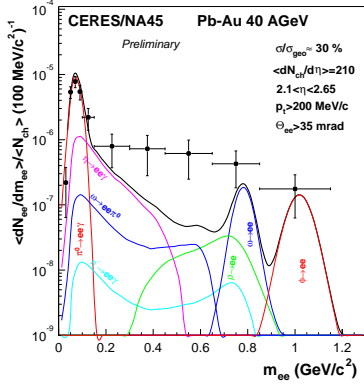


Figure 4. Invariant low-mass e^+e^- spectrum measured by CERES in 40 A GeV ²³ Pb-Au collisions. The figure also shows the summed (thick solid line) and individual contributions from hadronic sources.

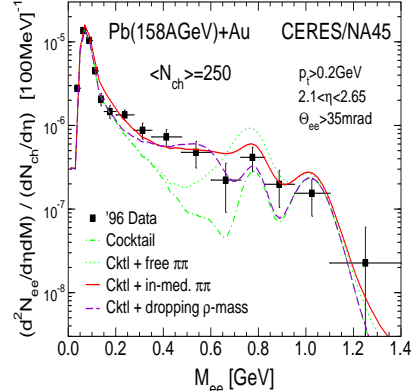


Figure 5. Comparison of CERES 96 results from Pb-Au collisions at 158 A GeV with various theoretical approaches (see text).

region after having regained their vacuum properties. The ω and ϕ mesons remain nevertheless important messengers: the undisturbed ω can serve as a reference and the ϕ with its $s\bar{s}$ content is a probe of strangeness production.

The CERES experiment has systematically studied the production of low-mass e^+e^- pairs, $m = 200 - 600 \text{ MeV}/c^2$, with measurements of p-Be (a very good approximation to pp collisions) and p-Au at 450 GeV/c ^{17,18}, S-Au at 200 GeV per nucleon ¹⁹, and Pb-Au at 158 GeV per nucleon ^{21,22} and 40 GeV per nucleon ²³. Whereas the p data are well reproduced by the known hadronic sources, a strong enhancement of low-mass pairs is observed both in the S and Pb data with respect to those sources, scaled to the nuclear case with the event multiplicity. Fig. 4 shows the preliminary mass spectrum from Pb-Au collisions at 40 A GeV with an enhancement factor of $5.0 \pm 1.5(\text{stat.})$ relative to the hadronic cocktail for masses $m > 200 \text{ MeV}/c^2$. With the large statistical uncertainty, this is consistent with the enhancement factor of $2.9 \pm 0.3(\text{stat.}) \pm 0.6(\text{syst.})$ obtained from the combined 95-96 Pb-Au data at 158 A GeV. Further studies on the latter demonstrate that the enhancement is more pronounced at low pair p_T and increases faster than linearly with the event multiplicity. In all cases, with the S and Pb beam, the enhancement sets at $m \geq 2m_\pi$.

The enhancement of low-mass dileptons has triggered a wealth of theoretical activity. Dozens of articles have been published on the subject. (For a comprehensive review see ²⁴). There is consensus that a simple superposition of pp collisions cannot explain the data and that an additional source

is needed. The pion annihilation channel ($\pi^+\pi^- \rightarrow \rho \rightarrow l^+l^-$), obviously irrelevant in pp collisions, has to be added in the nuclear case. This channel accounts for a large fraction of the observed enhancement (see line cocktail + free $\pi\pi$ in Fig. 5) and provides first evidence of thermal radiation from a dense hadron gas. However, in order to quantitatively reproduce the data in the mass region $0.2 < m_{e^+e^-} < 0.6$ GeV/c², it was found necessary to include in-medium modifications of the ρ meson. Li, Ko and Brown ²⁵, following the original Brown-Rho scaling ²⁶, proposed a decrease of the ρ -mass in the hot and dense fireball, as a precursor of chiral symmetry restoration, and achieved excellent agreement with the CERES data (see the line cocktail + dropping mass in Fig. 5).

Another avenue, based on effective Lagrangians, uses the broadening of the ρ -meson spectral function resulting from its propagation in the medium, mainly from the scattering of ρ mesons off baryons ²⁷, and achieves also an excellent reproduction of the CERES data (see line cocktail + in-medium $\pi\pi$ in Fig. 5). The success of these two different approaches, one relying on quark degrees of freedom and the other on a pure hadronic model, has attracted considerable interest raising the hypothesis of quark-hadron duality. Rapp provided empirical support to this hypothesis by showing that in a high density hadron gas the dilepton production rates calculated with the in-medium ρ -meson spectral function are very similar to the $q\bar{q}$ annihilation rates calculated in pQCD ²⁸.

Finally, it is interesting to note that the 40 A GeV data is also equally well reproduced by the dropping-mass and broadening scenarios ²³. Much better data are needed, in order to discriminate among the two. It is hoped that the last CERES run of year 2000 taken with an improved mass resolution of $\sim 2\%$ at the ω mass and good statistics should allow that.

4 J/ψ Suppression

The melting of charmonium states in a deconfined state of matter is one of the oldest signatures of QGP formation ²⁹ and has provided one of the most exciting sagas of the SPS programme. Already in the first runs with O and S beams, the NA38/NA50 experiment observed a suppression of J/ψ which immediately captured the interest ³⁰. Intensive theoretical efforts were devoted to explain the suppression within conventional physics and it soon became clear that all experimental data, including systematic studies of pp, pA and S-U collisions, can be reproduced by invoking the absorption in the nuclear medium of the $c\bar{c}$ pair before it forms a J/ψ , with an absorption cross section $\sigma_{abs} = 6.4 \pm 0.8$ mb ³⁰.

However, a different behavior is observed with the 158 A GeV Pb beam. Whereas peripheral collisions seem to follow the regular absorption pattern, an anomalously larger suppression occurs at more central collisions characterized by impact parameters $b < 8\text{fm}$ or $E_T > 40\text{GeV}$ which can be translated into a Bjorken energy density $\epsilon > 2.3\text{GeV/fm}^3$ (see Fig. 6³¹). The data in this figure exhibit a two-step suppression pattern which NA50 attributes to the successive melting of the χ_c and directly produced J/ψ mesons in a quark-gluon plasma scenario.

The same data normalized to the Drell-Yan cross section is shown in Fig. 7 as function of E_T . The two-step pattern can be discerned here at E_T values of ~ 30 and ~ 100 GeV. Most published calculations, based on conventional hadronic models including the effect of absorption by comovers, fail to reproduce the results as illustrated in the left panel of Fig. 7. The recent calculations of Capella et al.³² are in much better agreement with the data and fail only at the most central collisions (middle panel). On the other hand, quite good agreement over the whole E_T range is achieved by models assuming QGP formation (right panel)^{33,34}. The model of Blaizot et al. reproduce the data remarkably well by invoking J/ψ suppression whenever the energy density exceeds the critical value for deconfinement (first step) together with fluctuations of the transverse energy for the most central collisions (second step)³³.

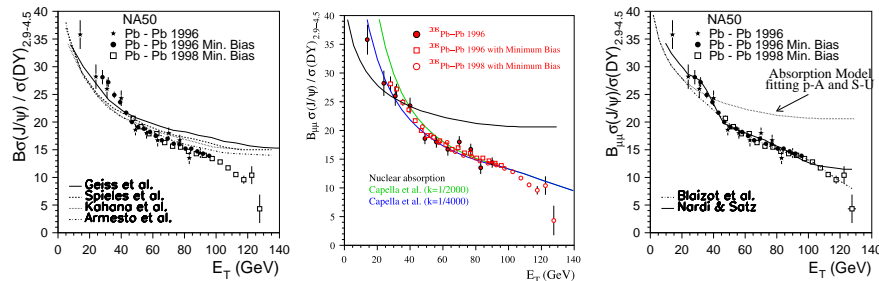


Figure 7. J/ψ over Drell-Yan cross section vs. E_T measured by NA50 in Pb-Pb collisions at $\sqrt{s_{NN}} = 17.2\text{ GeV}$ in comparison to various theoretical approaches using conventional physics (left and middle panels) and quark matter formation (right panel) (taken from³⁵).

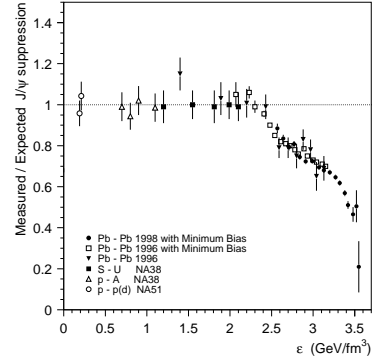


Figure 6. Measured over expected (assuming normal absorption cross section) J/ψ yield vs. energy density³¹.

5 Suppression of large p_T hadrons

With the energies available at RHIC, one order of magnitude higher than at the SPS, new channels and probes become accessible for diagnostic of matter under extreme conditions. In particular, the propagation in a dense medium of high p_T partons resulting from hard scattering and jet production in the initial phase of the collision, is an interesting question that has been extensively studied over the last decade ³⁶. Energy loss of the partons through gluon radiation has been predicted as a possible signature of deconfined matter. The phenomenon, commonly referred to as jet quenching, should manifest itself as a suppression of high p_T particles. Such a suppression has been observed already in the first low-luminosity RHIC run by the two large experiments STAR ³⁷ and PHENIX ³⁸ and certainly constitutes the most interesting result from RHIC so far. The suppression is evidenced by plotting the so-called nuclear modification factor³⁹ defined as the ratio of AA to pp p_T spectra, scaled by the number of binary collisions:

$$R_{AA}(p_T) = \frac{d^2\sigma_{AA}/dp_T d\eta}{\langle N_{bin} \rangle d^2\sigma_{pp}/dp_T d\eta}$$

In the absence of any new physics this ratio should be equal to 1 at the high p_T characteristic of hard processes. At low p_T , dominated by soft processes which scale with the number of participants, the ratio is expected to be lower, e.g. for central collisions $R_{AA}(0) \approx 0.5N_{part}/N_{bin} \approx 0.2$. The STAR and PHENIX results for central Au-Au collisions at $\sqrt{s_{NN}} = 130$ GeV are shown in Figs. 8 and 9 respectively. In both cases the pp data at 130 GeV were derived from interpolation of pp data ^{15,40,41} at lower and higher energies. STAR shows the ratio for negative hadrons and PHENIX for negative hadrons as well as identified π^0 . As expected, for low p_T the ratio is small, ≈ 0.2 . It raises with p_T , getting close to 1 and then falls off at higher p_T . The suppression appears to be stronger for π^0 than for charged particles although both are consistent within their large systematic errors. A similar suppression pattern appears when the ratio of central to peripheral collisions, each divided by its corresponding value of N_{bin} , is plotted as function of p_T ³⁸. This behaviour is in marked contrast to the observations in Pb-Pb and Pb-Au collisions at the SPS (the solid lines in Fig. 10 represent the band of uncertainty of the CERN results) where the ratio overshoots 1 and saturates at high p_T , like in pA collisions ³⁹, an effect known as the Cronin effect ⁴². The high p_T suppression observed at RHIC can be quantitatively reproduced in terms of jet quenching if an average energy loss of $dE/dx \approx 0.25$ GeV/fm is assumed within a parton model ⁴³. New RHIC data allowing to reach much higher p_T

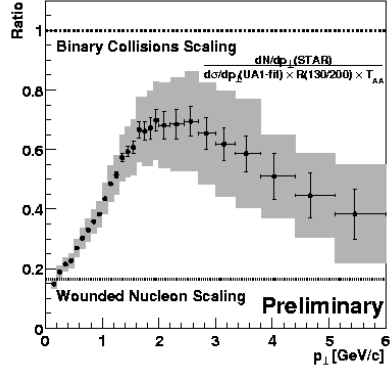


Figure 8. The ratio $R_{AA}(p_T)$ for negative hadrons measured by STAR in Au-Au collisions at $\sqrt{s_{NN}} = 130$ GeV ³⁷.

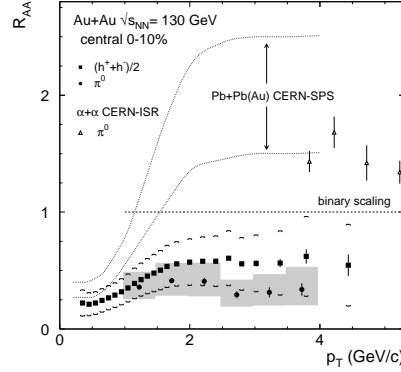


Figure 9. The ratio $R_{AA}(p_T)$ for negative hadrons and π^0 measured by PHENIX in Au-Au collisions at $\sqrt{s_{NN}} = 130$ GeV ³⁸.

values together with reference data on pp and pA measured within the same apparatus will be very valuable to consolidate these intriguing results.

6 Conclusion

In a relatively short run, the RHIC experiments have produced an impressive amount of results and much more is expected over the next years. The second RHIC run has just been completed with a recorded luminosity almost two orders of magnitude larger than in year-1. This, together with the still ongoing yield of interesting results from the SPS programme, places the field of relativistic heavy-ion collisions at a very unique phase with exciting physics prospects.

Acknowledgments

It is a pleasure to acknowledge support from the MINERVA Foundation and the US-Israel Binational Science Foundation.

References

1. F. Karsch, *Nucl. Phys.* **A698**, (2002) in press.
2. For a detailed survey of recent results see the Proceedings of Quark Matter 2001 in *Nucl. Phys.* **A698**, (2002) in press.
3. J.D. Bjorken, *Phys. Rev. D* **27**, 140 (1983).
4. X.N. Wang and M. Gyulassy, *Phys. Rev. Lett.* **86**, 3496 (2001).
5. B.B. Back et al., PHOBOS Coll., nucl-ex/0108009.
6. K. Adcox et al., PHENIX Coll., *Phys. Rev. Lett.* **87**, 052301 (2001).
7. D. Kharzeev and M. Nardi, *Phys. Lett. B* **507**, 121 (2001).

8. K. Adcox et al., PHENIX Coll., *Phys. Rev. Lett.* **86**, 3500 (2001).
9. X.N. Wang and M. Gyulassy, *Phys. Rev. D* **44**, 3501 (1991).
10. A. Capella and D. Sousa, *Phys. Lett. B* **511**, 185 (2001).
11. M.M. Aggarwal et al., WA98 Coll., *Eur. Phys. J.* **C18**, 651 (2001).
12. F. Antinori et al, WA97 Coll., *Eur. Phys. J.* **C18**, 57 (2000).
13. A. Milov for the PHENIX Collaboration, in 2.
14. G.J. Alner et al., UA5 Coll., *Z. Phys.* **C33**, 1 (1986).
15. C. Albajar, UA1 Coll., *Nucl. Phys.* **B335**, 261 (1990).
16. E.V. Shuryak, *Phys. Lett. B* **78**, 150 (1978).
17. G. Agakichiev et al., CERES Coll., *Eur. Phys. J.* **C4**, 231 (1998).
18. G. Agakichiev et al., CERES Coll., *Eur. Phys. J.* **C4**, 249 (1998).
19. G. Agakichiev et al., CERES Coll., *Phys. Rev. Lett.* **75**, 1272 (1995).
20. I. Ravinovich, for the CERES Coll., *Nucl. Phys.* **A638**, 159c (1998).
21. G. Agakichiev et al., CERES Coll., *Phys. Lett. B* **422**, 405 (1998).
22. B. Lenkeit, for the CERES Coll., *Nucl. Phys.* **A661**, 23 (1999).
23. H. Appelshauser for the CERES Coll., in 2.
24. R. Rapp and J. Wambach, *Adv. Nucl. Phys.* **25**, 1 (2000).
25. G.Q. Li, C.M. Ko and G.E. Brown, *Phys. Rev. Lett.* **75**, 4007 (1995).
26. G.E. Brown and M. Rho, *Phys. Rev. Lett.* **66**, 2720 (1991) and *Phys. Rep.* **269**, 333 (1996).
27. R. Rapp, G. Chanfray and J. Wambach, *Nucl. Phys.* **A617**, 472 (1997). and J. Wambach, *Nucl. Phys.* **A638**, 171c (1998).
28. R. Rapp, *Nucl. Phys.* **A661**, 33 (1999).
29. T. Matsui and H. Satz, *Phys. Lett. B* **178**, 416 (1986).
30. M.C. Abreu et al., NA38 Coll., *Phys. Lett. B* **449**, 128 (1999) and *Phys. Lett. B* **466**, 408 (1999).
31. M.C. Abreu et al., NA50 Coll., *Phys. Lett. B* **477**, 28 (2000).
32. A. Capella et al., *Phys. Rev. Lett.* **85**, 2080 (2000).
33. J.P. Blaizot et al., *Phys. Rev. Lett.* **85**, 4012 (2000).
34. M. Nardi and H. Satz, *Phys. Lett. B* **442**, 14 (1998).
35. P. Bordalo for the NA50 Coll., in 2.
36. X.N. Wang and M. Gyulassy *Phys. Rev. D* **44**, 3501 (1991) and *Phys. Rev. Lett.* **68**, 1480 (1992).
37. J. Harris for the STAR Coll., in 2.
38. K. Adcox et al., PHENIX Coll., *Phys. Rev. Lett.* **88**, 022301 (2001).
39. E. Wang and X.N. Wang, *Phys. Rev.* **C64**, 034901 (2001).
40. B. Alper et al., *Nucl. Phys.* **B100**, 237 (1975).
41. F. Abe et al., CDF Coll., *Phys. Rev. Lett.* **61**, 1819 (1988).
42. D. Antreasyan et al., *Phys. Rev. D* **19**, 764 (1979).
43. X.N. Wang in 2.